Sea level variations in the tropical Pacific Ocean during two types of recent El Niño events

Yi-Ting Chang [a], Ling Du [a,*], Shou-Wen Zhang [a], Peng-Fei Huang [a,b]

[a] Physical Oceanography Laboratory, Ocean University of China, PR China
[b] DaLian Naval Academy, PR China

ARTICLE INFO

ABSTRACT

Sea level variations in the tropical Pacific Ocean (TPO) exhibit the prominent periods of 30 and 52 months on interannual timescale, and the interannual variance illustrates the geographical distribution over the 1993–2010 period. The quasi-biennial amplitude is comparable to the seasonal variation in the east off the Philippine coast (EOP). The Central Pacific El Niño (CP El Niño) events have occurred frequently and comparably in the satellite altimetry era compared with the Eastern Pacific El Niño (EP El Niño), and the sea level varies closely related to the two types of El Niño events. A see–saw mode of sea level is dominant during the EP El Niño event, but a "shuttle" pattern towers mainly in the central equatorial Pacific during the CP El Niño events. The oceanic and atmospheric processes interpret the sea level evolution during the CP El Niño and the EP El Niño events. Sea level variations in the EOP are impacted by the local and remote responses of atmospheric wind fields. The remote effect caused by the westward Rossby wave dominates in the atmospheric contribution which is nearly twice the magnitude of the local Ekman pumping effect. The local wind contributes to sea level evolution primarily in the beginning of the El Niño events. The remote process of the Rossby wave persists in 35% of the three CP El Niño phases, while the predicted skill distribution, about 43—53%, maps geographical variability in the EP El Niño event.

1. Introduction

Sea level change has become an increasing concern worldwide not only because of its potential impact on people living in coastal regions and on islands, but also because it is an essential section of climate change. It is reported that sea level varies non-uniformly over multi-timescales including the secular change (Bindoff et al., 2007). The tropical Pacific has a conspicuous discrepancy, in which, the sea level is rising in the western Pacific but falling in the eastern Pacific in the satellite altimetry era (Cazenave et al., 2008). The tropical Pacific plays a crucial role in affecting the processes in the extra-tropical basins. It is the pronounced region of the ENSO phenomenon which may influence the high latitudes and the Indian Ocean through an oceanic and atmospheric bridge (Wang and Fiedler, 2006). Additionally, there are some important currents in this region, such as the North Equatorial Current (NEC), the South Equatorial Current (SEC), the North Equatorial Counter Current (NECC), the South Equatorial Counter Current (SECC) and the Equatorial Undercurrent (EUC). The NEC connects the subtropical gyre and the tropical gyre flows westward. Upon encountering the Philippine coast, the NEC bifurcates into the Mindanao Current and the Kuroshio Current. The

Kuroshio, one of the strongest boundary currents, transports moisture and heat from the equator to high latitudes. Thus, the bifurcation of the NEC provides an important indicator of mass and heat exchanges between the low and mid latitude North Pacific (Lukas et al., 1991; Fine et al., 1994). Another typical region in the tropical Pacific is the western Pacific Warm Pool (surface temperature above 28.5 °C), as it is closely associated with the regional and global atmospheric convection as well as rainfall (Wyrtki, 1989).

Former researches about sea level interannual variations focus on its contribution factors. The global mean sea level variations can be explained by the global terrestrial water storage variations (Llovel et al., 2011), the ocean mass change and the steric sea level (Willis et al., 2008; Llovel et al., 2010). It also showed a close connection to the ENSO phenomenon, with sea level rising (dropping) during El Niño (La Niña) (Nerem et al., 2010). Interannual variation in low latitude Pacific was closely related to the ENSO phenomenon. Using tide gauges along the coast of the Pacific, Gu and Li (2009) found that the interannual sea level variations in the Pacific were influenced by the ENSO. Their correlation coefficients were positive (negative) in the eastern (western) Pacific, and weakened with increasing latitude. The results, which were given by regression analysis with respect to the high-passed Multivariate ENSO index, indicated that the interannual sea level fingerprint mainly in the tropical Pacific was highly correlated to the ENSO events (Zhang and Church, 2012). During the El Niño event, sea level varied remarkably which could be influenced by the zonal wind stress in the tropical Pacific. The

correlation coefficients between sea level variation and equatorial currents were more than 0.6, which indicated that the sea level variation was influenced by wind field mainly through Ekman transport (Li et al., 2012). With a coupling climate model, Li et al. (2004) simulated that the Indonesian Through Flow could impact on sea surface height variation. The steric sea level played an important role in the north Pacific on the interannual timescale (Xu et al., 2010).

There are two types of El Niño events in the tropical Pacific, and the regional ocean dynamics as well as the thermal structure is different during the two events (Ashok et al., 2007; Weng et al., 2007). The events, such as the sea surface temperature anomaly (SSTA) in the central Pacific flanked by anomalous cooling in both sides of the equator, had been observed frequently in the past three decades (Lee and McPhaden, 2010). This phenomenon had been viewed as a different El Niño event named El Niño Modoki (Ashok et al., 2007), Central Pacific El Niño (Kao and Yu, 2009), and Warm Pool El Niño (Kug et al., 2009), and the two types of El Niño were linearly independent (Li et al., 2010). Different with the EP El Niño, the maximum SSTA occurred mainly in the central Pacific in the boreal summer (Ashok and Yamagata, 2009). Additionally, anomalous subsurface temperature, precipitation and atmospheric vertical motion shifted to the west during CP El Niño (Kug et al., 2009). A double-cell Walker circulation caused an easterly wind anomaly to occur in the east while a westerly wind anomaly occurred in the west over the tropical Pacific during CP El Niño (Weng et al., 2007). After the CP El Niño event, it was difficult to exhibit the corresponding La Niña event (Kao and Yu, 2009; Kug et al., 2009). The influence of the two types of events was opposite in New Zealand, Japan and the western coast of the United States on a seasonal scale (Ashok et al., 2007). A stronger atmospheric circulation could enhance western North Pacific summer monsoon in South China Sea in CP El Niño (Chang et al., 2008). The teleconnection pattern between the two kinds of El Niño events and SPCZ was remarkably different; it became strong in CP El Niño (Garfinkel et al., 2012). The observed warming in West Antarctica was significantly affected by the trend of central tropical Pacific warming (Ding et al., 2011). The El Niño pattern suppressed the Atlantic tropical cyclone activity. The main developed SST region played a more important role since the restraining effect was diminished during CP El Niño (Larson et al., 2012).

Previous studies about interannual variations are mainly issued about global mean and coastal sea levels; the spatial characteristic has rarely been illustrated. This paper will focus on the geographical distribution of interannual sea level variations in the tropical Pacific. Furthermore, the discrepancy of the evolutions between the two types of El Niño events is discussed with the oceanic and atmospheric processes. Besides, this paper tries to interpret the sea level variations in the atmospheric wind dynamic process while the variations used to be mainly concentrated on steric contribution. The local and remote skills of wind field are given in order to evaluate the atmospheric predictability during the evolution of the two types of El Niño events in the east off the Philippine coast (EOP).

2. Data

Sea level anomaly (SLA) data used in this study is derived from Archiving, Validation, and Interpretation of Satellite Oceanographic (AVISO) data. The 1/3° × 1/3° gridded monthly datasets are computed with respect to a seven-year mean during January 1993 and December 1999. The SLA datasets were retrieved from multiple satellites (TOPEX/Poseidon, Jason-1, Jason-2, ERS, Envisat) with the same ground tracks. Instrument corrections and geophysical correction are applied to the raw altimeter data. We extract the data from Jan. 1993 to Mar. 2010 to analyze the interannual variation of sea level in the tropical Pacific Ocean (TPO).

Objective three-dimensional ocean temperature fields, noted as Ishii datasets are provided by the Japan Marine Science and Technology Center. This version 6.12 is objectively analyzed based on the measured data from the latest World Ocean Database (WOD09), Global Temperature and Salinity Profile Project (GTSPP) and expendable bathythermographs (XBT). ARGO profiling buoy data has also been used in the last several years. The updated XBT depth bias correction is applied and several minor bugs are fixed in this version. It is available at 1° × 1° horizontal resolution and has 24 standard levels in the upper 1500 m. The 20 °C isotherm of temperature fields is related to the largest temperature gradient in the tropical Pacific based on the former studies, so it is used to represent the ocean thermocline.

The reanalysis of zonal and meridional wind stresses are obtained from the European Centre for Medium-Range Weather Forecasts (ECMWF) with a horizontal resolution of 1° × 1°. A new operational ocean analysis/reanalysis system (ORA-S3) has been introduced in this datasets. The assimilation system is updated mainly in this version. Through quality controlling, the observed data in the upper 2000 m is assimilated. Assimilation of altimetry sea level anomalies, global sea level trends and salinity data is an innovative point. In order to reduce spurious climate variability brought from the ocean reanalysis, an on-line bias-correction algorithm and five simultaneous analyses are performed in this system (Balmaseda et al., 2008). The dataset is used in the Markov model and the 1.5-layer reduced-gravity model to calculate the sea level variations affected by wind field.

3. Sea level variation in the tropical Pacific

3.1. The characteristics of the interannual sea level variation

Sea level variations illustrate the obvious interannual variability with spatial non-uniform features in the TPO (Fig. 1). The low-frequency time series whose period is larger than one year are obtained by the low-pass filtered SLA. The spectrum energy ratio denotes that the interannual variations account for the low-frequency series after a significant test. Interannual sea level variation is found in the TPO with its deviation larger than 5 cm expect for several blank regions. The spatial distribution of the interannual deviation is performed geographically, which is similar to the sea level secular trend reported in the former researches. The interannual variability occurs remarkably in the western Pacific Warm Pool and the eastern equatorial Pacific. In the core area of the western Pacific Warm Pool (surrounded by 28.5 isotherm of May), the deviation is almost larger than 5 cm, especially in the east off the Philippines and New Guinea.

The significant periods are focused on 30 months (quasi-biennial) and 52 months in the low-frequency series, and the amplitudes corresponding to the two periods exist mainly in the western Pacific Warm Pool, central and eastern equatorial Pacific (Fig. 2). The stochastic dynamic method (Epstein, 1969) can distinguish the different fluctuations of a series. Estimated by maximum entropy spectrum, it could distinguish the precise and primary sea level variations on different time scales according to a relevantly shorter timeseries (Tian et al, 1993). Based on the stochastic dynamic method, the statistical results of the significant periods in low-frequency in the TPO are shown in Fig. 2a. The probability density functions (PDF) shows a bimodal structure over the seven significant periods. The first two significant interannual oscillations in the PDF occupy 39% and 21% probability of the total low-frequency series. The two components are analyzed further as their big proportion (60%). The quasi-biennial oscillations exist mainly in the EOP where NEC bifurcates, and east of the dateline in the equatorial Pacific noted the Nino4 and Nino3 regions (Fig. 2b). Moreover, the oscillations are out of phase in the two regions (figure not shown). The pattern of quasi-biennial oscillation is extremely similar to the power spectrum, STD pattern and composite pattern of the CP El Niño (Fig. 5b). It is probably related to the frequent CP El Niño recently in the central Pacific, while it is related to the edge of the Warm Pool which moves north and south in the EOP. The amplitude of quasi-
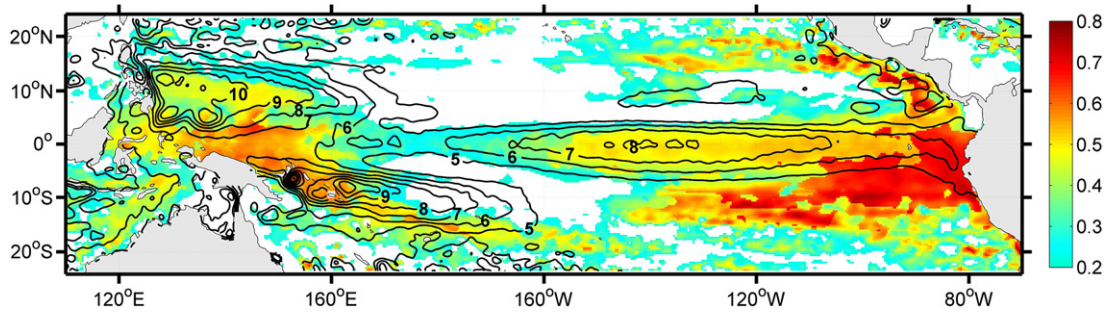
Fig. 1. Geographical distribution of the SLA spectrum energy ratio and its standard deviation. The shading denotes the ratio of the power spectrum at 95% statistical confidence level. Blank indicates no significant interannual variation. Contour interval of the standard deviation is 1 cm.

biennial oscillation in the EOP, about 7 cm, is nearly equal to the local seasonal oscillation. The interannual oscillation (52 months) is located in the eastern equatorial Pacific and in the east off Indonesia in the Warm Pool (Fig. 2c). Agreeing with the pattern of SSTA, it also resembles the composite pattern of SLA during the EP El Niño (Fig. 5a). It implies that sea level variation is different between the two types of El Niño events. Compared with the patterns of the quasi-biennial and the interannual variations (52 months), the predominant period is quasi-biennial in the EOP, while both two periods are significant in the equatorial Pacific. In addition, the 69 month oscillation is located in the south of the Warm Pool with the maximum amplitude nearly 7 cm (figure not shown).

3.2. The relationship between regional SLA and El Niño events

According to the magnitude of interannual sea level variations (Fig. 2), three special regions are selected in this part: the NEC bifurcation region (NECB, 130°E–150°E, 10°N–15°N), the central equatorial Pacific (CEP, 160°E–150°W, 5°S–5°N) and the eastern equatorial Pacific (EEP, 150°W–90°W, 5°S–5°N). The position of three regions is shown in Fig. 2b. The SLA series in these regions with the Nino3 index and ENSO Modoki index (EMI) are shown in Fig. 3. The procedure for calculating EMI is presented in Section 4.

The sea level variations are correlated with El Niño events in the selected regions (Fig. 3). The sea level in the NECB is negatively correlated with the Nino3 index, which indicates that the sea level drops (rises) during EP El Niño (La Niña). Furthermore, a similar result can be obtained between the NECB and the EMI during CP El Niño. The sea level in the NECB drops when the NEC bifurcation moves northward and vice versa. The same conclusion was drawn by Qiu and Chen (2010). The sea level in the EEP and the CEP varies synchronously in the CP El Niño. However it has a phase lag between the two regions during the EP El Niño. Except for the edge of the Warm Pool, sea level went down significantly during the 1997/98 EP El Niño event, while the minimum sea level was delayed by 1–2 months in the different belts from north to south (figure not shown).

4. Interannual sea level variations during the two El Niño events

Based on the objective sea surface temperature dataset, the two types of El Niño events are distinguished statistically. Sea level variations during the corresponding El Niño events are analyzed in this section. Furthermore, we find a relationship between sea level variation and wind field as well as vertical thermal structure on interannual timescale.
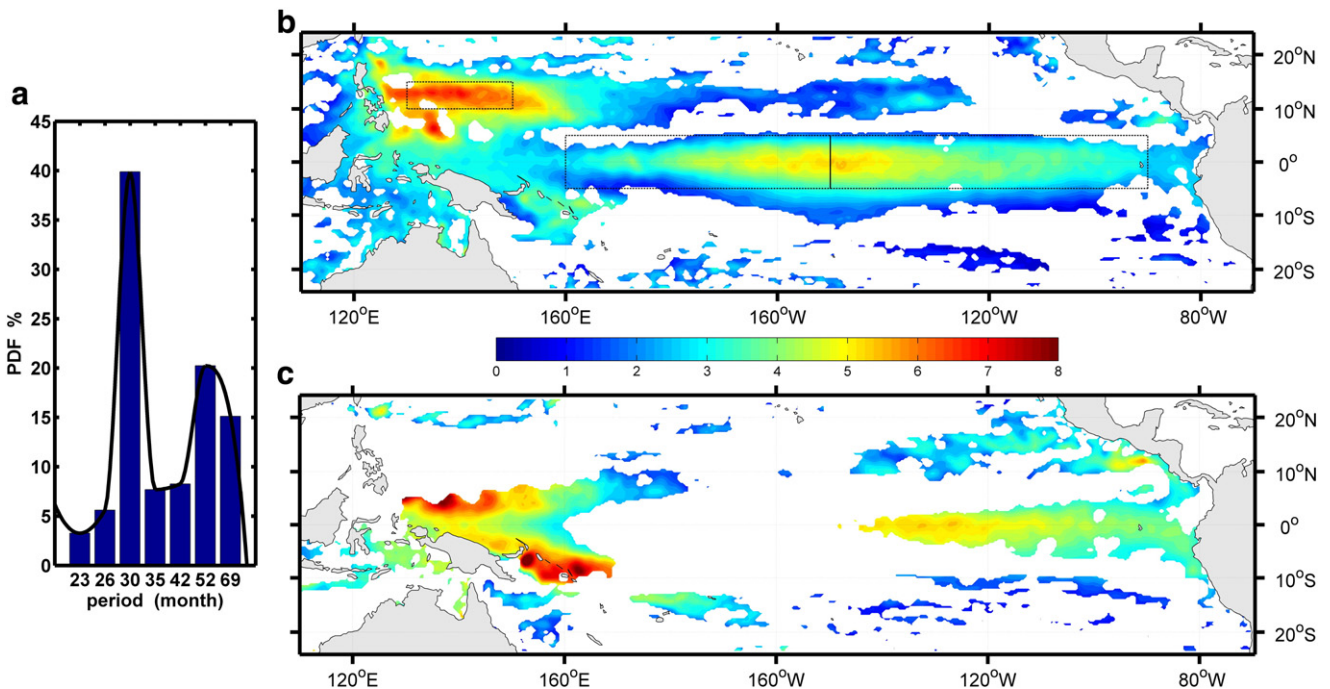
Fig. 2. The (a) probability density functions of the significant periods and the geographical distribution of amplitudes (unit: cm) on (b) 30 months and (c) 52 months.
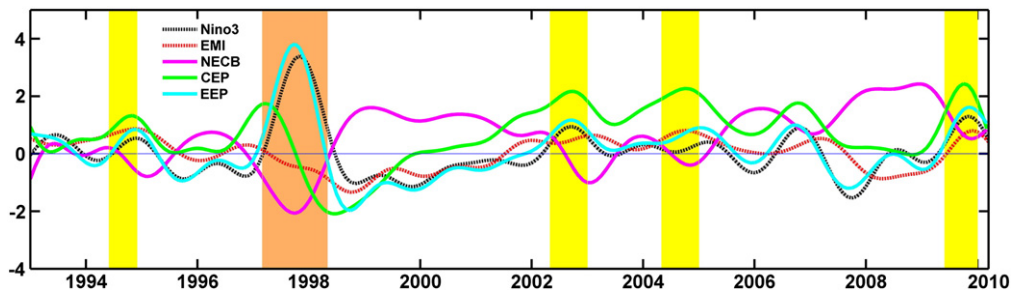
Fig. 3. Normalized series of SLA (14 months low-pass filtering) in the three selected regions with the Nino3 index and EMI. The yellow and orange blocks cover the CP El Niño event and the EP El Niño event.

4.1. Statistics of El Niño events

The zonal tripole pattern of the SSTA field in the tropical Pacific is robust, such as the warmer region in the central equatorial Pacific sandwiched by the cooler region in the eastern and western parts. Based on the objective SSTA in the TPO deriving from the Ishii datasets, the sandwich structure is illustrated by the EMI. The EMI is calculated by using the SSTA over the three regions, as region A (165°E–140°W, 10°S–10°N), B (110°W–70°W, 15°S–15°N) and C (125°E–145°E, 10°S–20°N), which are similar to Ashok et al. (2007). The SSTA time series are obtained by removing the seasonal signal from the monthly SST data.

Statistic of the EP El Niño and CP El Niño events is conducted by the Nino3 index and EMI. An EP El Niño event is defined conventionally when the Nino3 index exceeds 0.5 at least 6 consecutive months. Taking the definition of EP El Niño into consideration, a CP El Niño event is titled when the EMI is warmer than 0.5 times its standard deviation for 6 continuous months. Monthly geographical distribution of SSTA in the TPO is used to verify the classification elaborately, whether the warmer SSTA occurs mainly in the eastern Pacific during the EP El Niño event, and the warmer SSTA emerges in the central equatorial Pacific sandwiched by anomalous cooling in both sides during the CP El Niño event.

The CP El Niño event is found statistically to be more frequent compared with the EP El Niño event during the last two decades (Fig. 4). 21 El Niño events have been found in the past 60 years, including 11 EP El Niño events and the alternating 10 CP El Niño events. Before the 1980s, CP El Niño events have occurred only one time during every decade, while they have taken place six times in the recent twenty years. Conversely, the occurrence of EP El Niño events decreased. The strongest 1997/98 El Niño event in the 20th century has occurred in the satellite altimetry era. Meanwhile the CP El Niño events have come up frequently and comparably in the era. Thus, the 97/98 El Niño is selected as the typical EP El Niño event, and the CP El Niño events during 1994/95, 2002/03, 2004/05 are chosen for comparison (due to the limitations of dataset records, the 2009/10 event has not been chosen). The composite period of the EP El Niño

is May 1997 to May 1998 and that of the CP El Niño is July to the next March.

As mentioned above, the SSTA distribution exhibits a unique pattern in CP El Niño events, formally as a sandwich structure which can be pictured as a "cooling–warming–cooling" from east to west in the equatorial Pacific. The frequent occurrence of the SSTA sandwiched structure might revise the air–sea interaction background, and vary the corresponding ocean currents of ocean general circulation in the tropical basin. Additionally, through atmospheric wind field and relevant Rossby wave, it would influence the variations in the regional ocean dynamic processes and the exchange between tropical and extra-tropical ocean. Moreover, the interannual sea level variations display a significant difference between the two types of El Niño events in the TPO (shown in Section 4.2).

4.2. Interannual sea level variation

The patterns of the interannual sea level variations during the two types of El Niño events are remarkably different, especially in the central equatorial Pacific and Warm Pool (Fig. 5). The seesaw pattern of SLA during the EP El Niño event is predominant, which is similar to the SSTA pattern. Meanwhile the seesaw pattern pictured reversely to the reported sea level trend in the former studies. The seesaw exhibits the sea level rising in the eastern Pacific and declining in the Warm Pool. The extent and intensity of sea level rising and dropping are comparable, and the sea level tilts with the discrepancy up to 46 cm in the Pacific basin. Straddled in the rising region in eastern Pacific, sea level decline emerges in the Warm Pool especially in the EOP and the South Pacific Convergence Zone (SPCZ). Compared with the strongest EP El Niño event in the 20th century, the equatorial SSTA varies weakly in the CP El Niño events during the first decade of the 21st century. In the CP El Niño events, the extent of sea level rising and decline decreases 20% and 60% respectively, while the intensity of SLA reduces to half. Sea level rising mainly towers in the central equatorial Pacific, while the fall area shrinks to the EOP. The geographical distribution resembles the amplitude pattern of quasi-biennial oscillation in the TPO (Fig. 2b). It indicates that the quasi-biennial variation is tightly linked
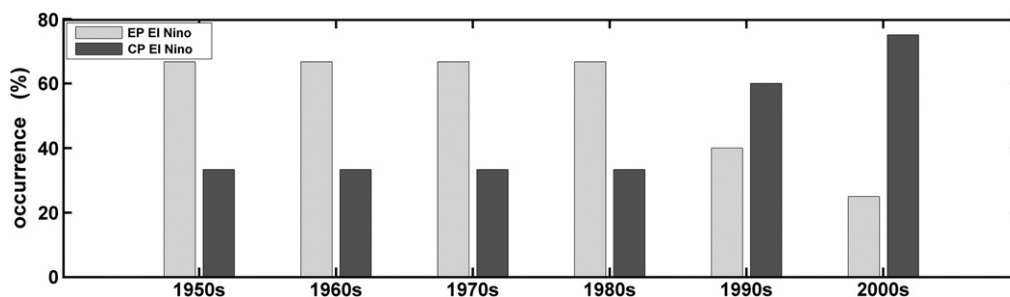
Fig. 4. The occurrences of El Niño events in the last six decades. Dark gray bar denotes the EP El Niño events and light gray bar denotes the CP El Niño events.
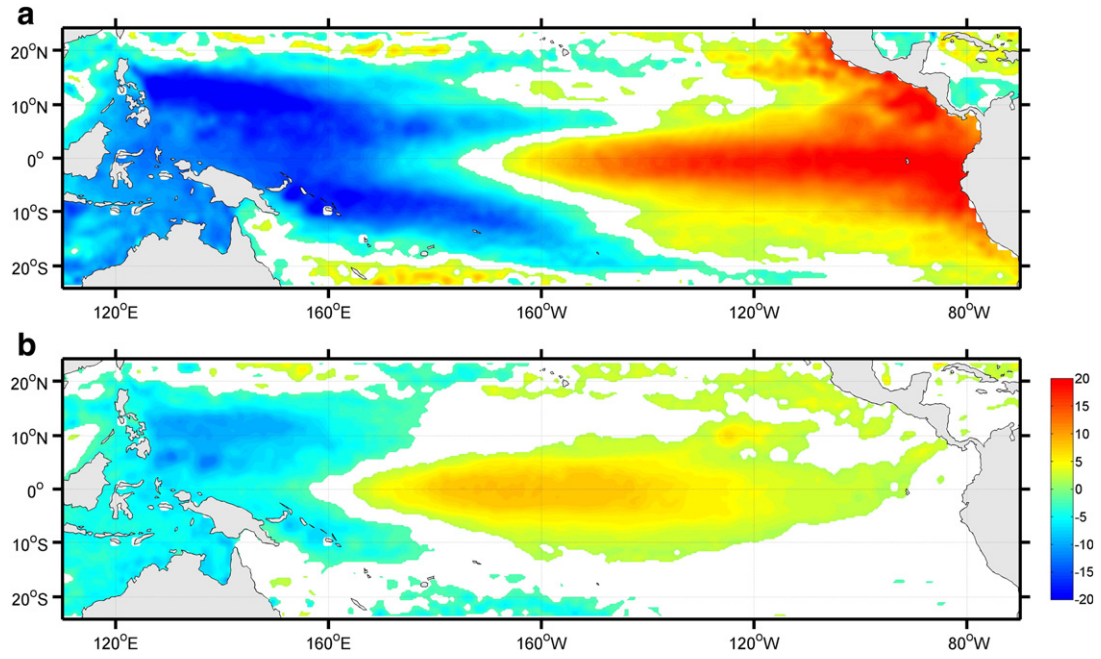
Fig. 5. Composite SLA (unit: cm) during (a) the EP El Niño event and (b) the CP El Niño events. Values above 95% confidence level of the *T*-test are shaded.
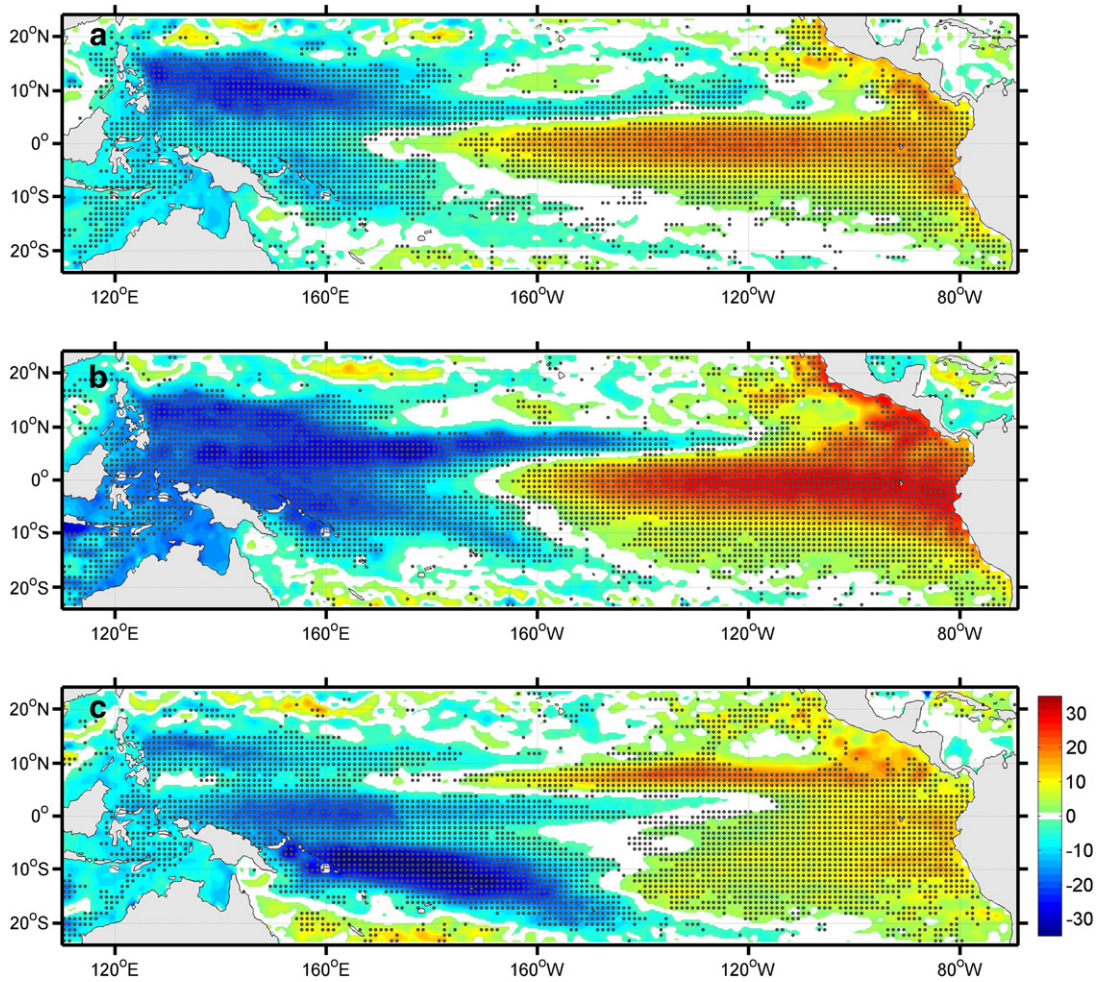

Fig. 6. Composite SLA in the (a) developing, (b) mature and (c) decaying phase in the EP El Niño event. Gray dot denotes the correlation which is significant between SLA and heat content at 99% significant level.

to the frequent CP El Niño events. The composite SLA during the EP El Niño and CP El Niño are similar to the principal patterns of observed rainfall (Cai et al., 2012), which suggests that the swing of SPCZ may related to the El Niño events. The sea level variations in the EOP during both two types of events are similar, which implies that it is a typical region which has an interannual signal.

The different evolution (the classification of the evolution is seen in Section 4.3) of sea level variations in the eastern and western Pacific is manifested during the EP El Niño event (Fig. 6). That is the sea level first rises and then drops in the eastern Pacific while an opposite evolution occurs in the EOP. The most two remarkable regions of SLA are located in the EOP and east of dateline in the equatorial Pacific in the developing phase. When it comes to the mature phase, the declining area expands to the whole Warm Pool and the rising area withdraws eastward. Up to the decaying phase, the low sea level is mainly in the SPCZ. Sea level variations between the EOP and the CEP display the different evolutions during the CP El Niño events (Fig. 7). Sea level rises (drops) firstly and then drops (rises) in the CEP (EOP). Moreover, the sea level changes locally and seems to not propagate.

4.3. The relevant oceanic and atmospheric processes

The EMI could not reflect the evolution of the CP El Niño events properly as it has a bimodal structure in August and next February (figure not shown). The selected CP El Niño events have been divided into three phases using Nino4 index noted as the developing, mature and decaying phase. And the similar classification is adopted in the EP El Niño event using Nino3 index.

During the evolution of the CP El Niño events, sea level variations in the CEP and EOP are significant. In the CEP, the weakened wind divergence is conducive to the sea level rising in the developing phase. Up to the mature phase, the divergence weakens further, which would result in the rising of regional sea level. Additionally, the extent of rising extends to the EEP owing to the divergence signal which moves eastward. Then, sea level drops due to the strengthened divergence in the equator from the mature to the decaying phase. In the EOP, atmospheric convergence weakens persistently from the developing to the decaying phase, and sea level drops except for the decaying phase. It suggests that sea level variation has relationship with the local wind field, while it is speculated that the different circumstance in the decaying phase might be explained by the atmospheric circulation above EOP. The detailed analysis is shown in Section 5. The similar evolutions are found in the eastern tropical Pacific and EOP during the EP El Niño event.

There is an oceanic and atmospheric response associated with the sea level variations in the El Niño events. What the easterly wind anomaly in the eastern Pacific combines with the westerly wind anomaly in the western Pacific would cause the atmospheric convergence mainly near the dateline in the equatorial Pacific during the CP El Niño events (Fig. 8b). Induced deepened thermocline occurs in the CEP. The thermocline flattens with the maximum variability of 15% in
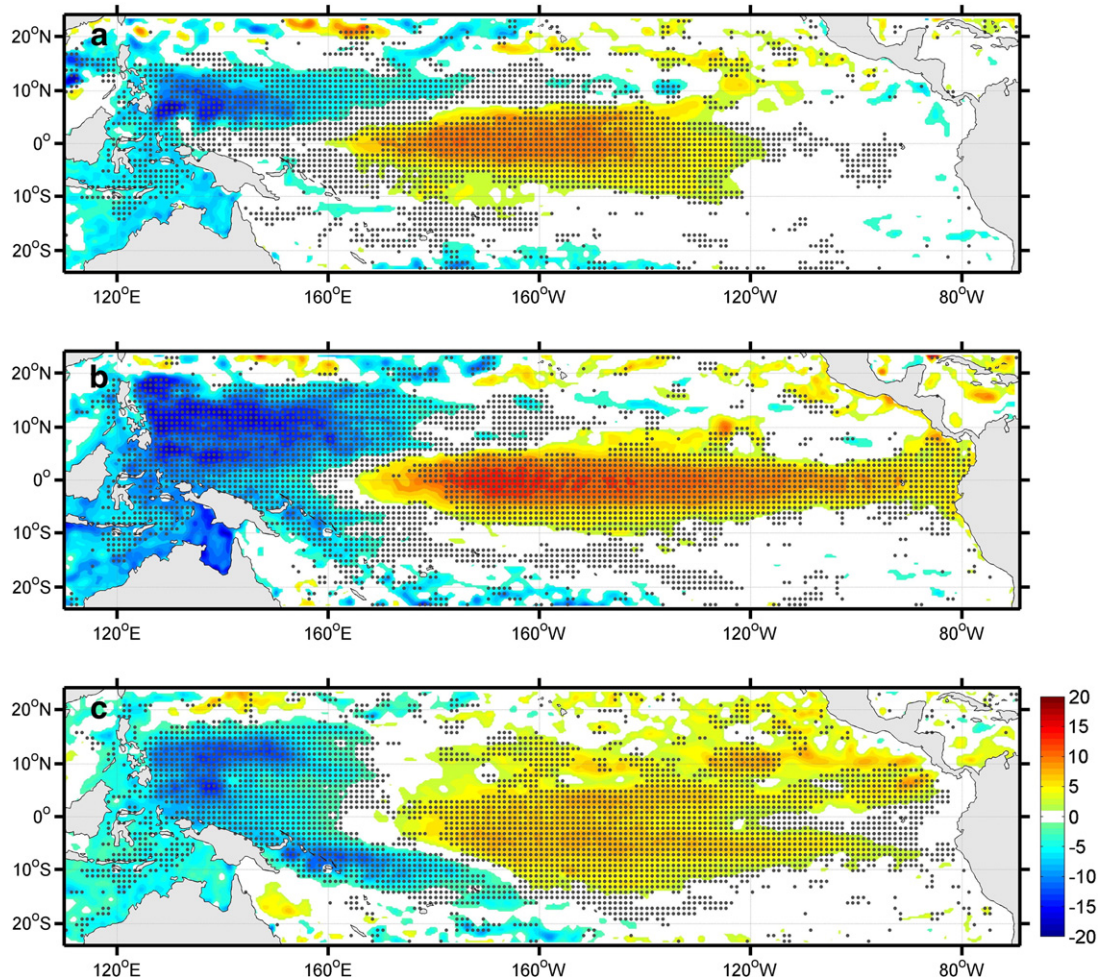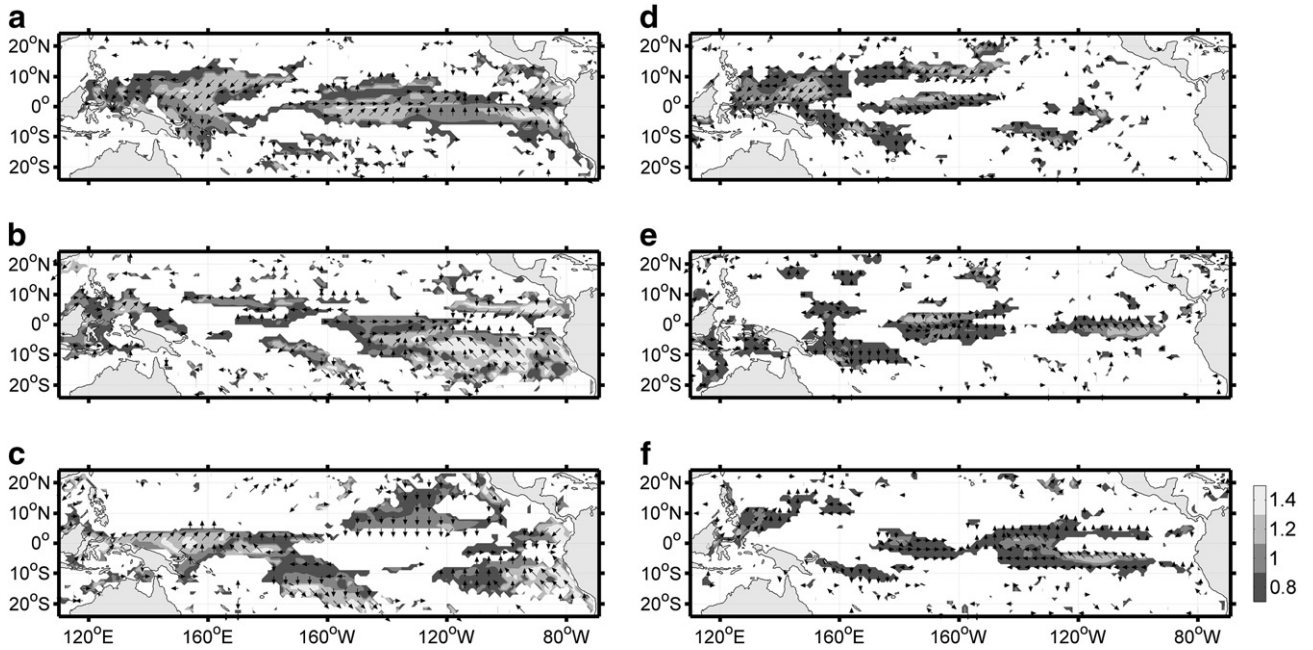

Fig. 7. Same as Fig. 6 but for the CP El Niño events.

Fig. 8. Correlation vector and its magnitude (shading) between SLA and wind stress during three phases in (a–c) the EP El Niño event and (d–f) the CP El Niño events. The correlation coefficients pass the 95% significant level test. East/west component indicates the correlation between SLA and zonal wind stress, and north/south component denotes the correlation between SLA and meridional wind stress.

the mature phase compared with that in the EP El Niño event. Associated with intensified stratification there, the vertical convection weakens. In addition to the remarkable warm anomaly in the subsurface and the anomalous warm ocean heat content, sea level rises in the CEP. On the contrary, the wind divergence anomaly shallows the thermocline in the EOP. The shoaled thermocline, whose maximum variance is up to 7% in the mature phase compared with the EP El Niño, intensifies the vertical mixing. The anomalous cold water in the subsurface is taken up to the surface which causes the whole water column to cool and the heat content to decrease. These processes all contribute to the declining sea level. The anomalous atmospheric divergence fields are stronger during the EP El Niño event. Occurring mainly in the EEP and EOP, the similar processes are generated due to the wind field effect.

The heat content in the tropical Pacific shows a lead/lag relationship with that in the NECB as well as in the western equatorial Pacific (WEP). The result indicates a propagation phenomenon (figure not shown). If the heat content anomaly occurred in the NECB, it would move southward to the WEP after two months. Superposing the local anomaly, the intensive heat content extends eastward across the Pacific basin. 14 months later, the heat content will reach the east side. In another

word, such a process would take around 16 months to propagate the heat content from the NEC bifurcation region to the eastern Pacific. As the negative heat content anomalies in the NECB and WEP regions are not pronounced during the CP El Niño events, the eastward anomalies are too weak to form the corresponding Central Pacific La Niña.

5. Effect of wind-forcing in the EOP

The altimetric SLA indicates that the significant interannual sea level variation occurs in the EOP. This region just located at the crossroads of the subtropical and tropical gyre. The NEC bifurcation associated with the two gyres provides an important approach for mass and heat exchange between low and mid latitudes. Furthermore, the heat content near the NECB might be a clue to the lack of Central Pacific La Niña in the former section. Due to the importance of this region, the relationship between interannual sea level variation and atmospheric wind field in the EOP (130°E–180°E, 8°N–16°N) needs further discussion.

The atmospheric wind field impacts on sea level variation by two approaches. One is the Ekman pumping influenced by local wind curl (referred to the local effect), that is, the sea level drops (rises) as the wind diverges (converges) (Lagerloef, 1995; Stammer, 1997). The
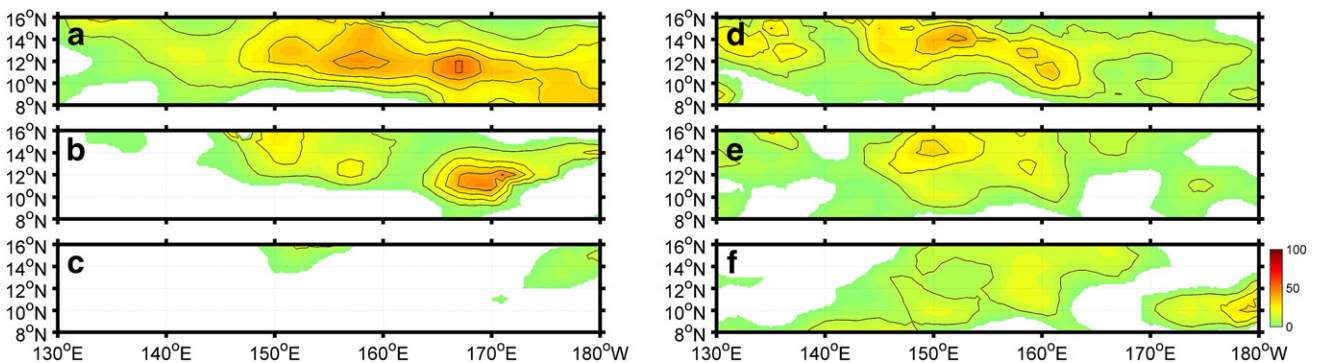
Fig. 9. Geographical distribution of the local effect ($\varepsilon^{-1} = 30$ days) in the three phases during (a–c) the EP El Niño event and (d–f) the CP El Niño events.

Table 1
the predictive skill (mean and standard deviation) of the local effect (S_L) in different phases of the El Niño events.

El Niño event		S_L (%)	
		$\varepsilon^{-1} = 30$ days	$\varepsilon^{-1} = 60$ days
EP El Niño	Developing	19 ± 12	28 ± 17
	Mature	13 ± 10	21 ± 15
	Decaying	5 ± 4	12 ± 7
CP El Niño	Developing	14 ± 9	20 ± 13
	Mature	11 ± 7	16 ± 11
	Decaying	9 ± 5	14 ± 7

Table 2
Same as Table 1 but for the remote effect (S_R).

El Niño event		S_R (%)
EP El Niño	Developing	41 ± 20
	Mature	56 ± 22
	Decaying	50 ± 25
CP El Niño	Developing	35 ± 15
	Mature	35 ± 12
	Decaying	36 ± 17

other approach is the westward Rossby wave inspired by the wind field east of the analyzed region (referred to the remote effect) (Qiu, 2002; Qiu and Chen, 2010).

Markov model (Lagerloef, 1995) is used to find the sea level variation due to local Ekman pumping.

$$\frac{\partial h_{ek}}{\partial t} = -\frac{g' curl\tau}{\rho_0 gf} - \varepsilon_1 h_{ek}. \tag{1}$$

1.5-Layer reduced-gravity model is taken to obtain the sea level variation introduced by the Rossby wave.

$$\frac{\partial h_r}{\partial t} - C_R \frac{\partial h_r}{\partial x} = -\frac{g' curl\tau}{\rho_0 gf} - \varepsilon_2 h_r \tag{2}$$

where C_R is the long baroclinic Rossby wave speed, f is Coriolis parameter, ρ_0 is the reference density, g is gravity constant, g' is reduced gravity, $curl\tau$ is the wind curl anomaly, ε_1, and ε_2 are the Newtonian dissipation rates. The parameter values are adopted: $g' = 0.03$ m/s^2, $\rho_0 = 1024$ kg/m^3, $\varepsilon_1^{-1} = 30$ days or 60 days, $\varepsilon_2^{-1} = 2$ years. The different value of ε is because of the different timescales of the two approaches.

The predictive skill (Qiu, 2002) of the wind field by the local and remote processes is defined by

$$S = 1 - \frac{<(h_o - h_m)^2>}{<h_o^2>} \tag{3}$$

where h_o is the observed sea level anomaly, h_m is the modeled sea level anomaly which refers to h_{ek} and h_r in Eqs. (1) and (2), and angle brackets denote the temporal average of the sea level anomaly. Based on the predictability of the wind field to the sea level variation, we focus on the modeled sea level anomaly which is less than the altimetric SLA. The local (remote) hindcast skill, named as S_L (S_R), implies the contribution that the modeled anomaly accounts for the interannual sea level variance.

Compared with the EP El Niño, the local predictive skill is smaller during the CP El Niño events (Fig. 9, Table 1). The local wind fields influence the sea level variation remarkably with the largest S_L in the developing phase, even more than that in the mature phase. It indicates that the local atmospheric wind field contributes to sea level evolution mainly in the very beginning of the El Niño events. The contribution decreases with the evolution of both two El Niño events. The discrepancy of S_L appears obviously in the decaying phase. The Ekman pumping is illustrated to have no contribution in the decaying EP El Niño event while it still contributes to sea level variation during the decaying CP El Niño. The Newtonian dissipation term is the principal factor to determine the timescale of the local atmospheric contribution. The faster dissipation occurs, the smaller influence appears (Table 1).

Atmospheric wind fields influence the regional sea level evolution mainly by the Rossby wave process during the El Niño events (Fig. 10, Table 2). S_R is larger than S_L in the corresponding phase. Similar to the local effect, the remote process contributes less during the CP El Niño events. The contribution of the Rossby wave process persists in one third of the three CP El Niño phases, while it varies from 43 to 53% in the EP El Niño events. The geographic distribution of S_R distinguishes strikingly in the two El Niño evolutions. The remote process affects the interannual sea level variation continuously in the CP El Niño events. Comparatively, the distribution of S_R maps the geographical variability in the EP El Niño. The large S_R becomes extensive and moves westward from the developing to the mature phase, and then withdraws northwestward with the value of 51% in the decaying EP El Niño event.

6. Summary

In this study, interannual sea level variation in the tropical Pacific Ocean is conducted in the past 17 years by satellite altimetry data from Jan. 1993 to Mar. 2010. The significant interannual signal is obtained by stochastic dynamic method in the TPO. The interannual variations map spatial non-uniform features with two prominent periods at 30 and 52 months, which account for 60% among the seven periods. The large interannual amplitudes mainly locate in the east off the Philippine coast and the equatorial Pacific. The quasi-biennial oscillation occurs obviously in the EOP, and its amplitude, up to 7 cm, is comparable to that of seasonal variation. Sea level variations exhibit a relationship with El Niño events compared with the Nino3 index and the ENSO Modoki index.
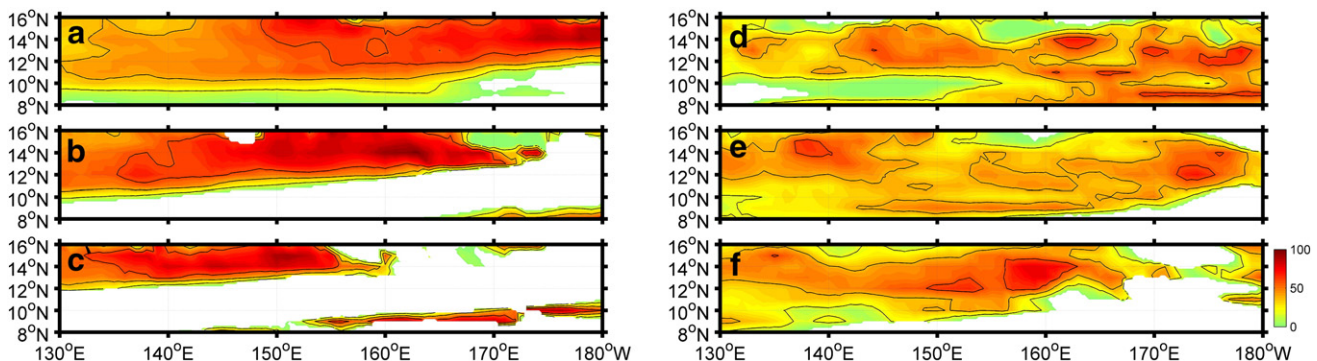

Fig. 10. Same as Fig. 9 but for the remote effect.

It is found that the CP El Niño events have occurred frequently and comparably in the last decade with statistical SSTA in the TPO, thus one EP El Niño event and three CP El Niño events are selected in the satellite era. The composite analysis is employed to obtain the discrepancy between the two types of El Niño events. The composite SLA illustrates the remarkable difference geographically. A see-saw mode is dominant during the EP El Niño event with the maximum anomaly up to 22 cm in eastern tropical Pacific, and the minimum anomaly about −24 cm in the western Warm Pool. In contrast, a "shuttle" pattern of the positive anomaly towers in central equatorial Pacific, with the largest value nearly 9 cm, in the CP El Niño. The sea level varies with the evolution of El Niño events, such as a rise–drop pattern in the EEP (CEP) and a drop–rise mode in the EOP (EOP) during the EP El Niño (CP El Niño).

The oceanic and atmospheric processes interpret the sea level evolution in the two types of El Niño events. It is found that the anomalous wind fields converge (diverge), the thermocline deepens (shoals), the oceanic stratification strengthens (weakens), and the vertical mixing becomes tender (intensive), combining with the warm (cool) temperature anomaly in the subsurface and the positive (negative) heat content anomaly, which contribute to the sea level rising (falling). Heat content shows the phenomenon like propagation from the NECB and WEP regions eastward to the east Pacific. Since the negative heat content anomalies in the NECB and WEP are not strong enough, it might not be favorable for the Central Pacific La Niña occurrence.

Interannual sea level variation has a relationship with the atmospheric wind field by local and remote processes in the EOP. Using the Markov model and the 1.5-layer reduced-gravity model, the local contribution influenced by the local Ekman pumping and the remote process induced by the westward propagating Rossby wave are shown respectively. The two effects have a striking discrepancy between the two types of El Niño events. The effect caused by the Rossby wave is dominant compared with the local Ekman pumping effect. Meanwhile the wind field effects during the EP El Niño are larger than that in the CP El Niño events. The local atmospheric wind contributes to sea level evolution mainly in the very beginning of the El Niño events. The Newtonian dissipation term is the principal factor to determine the timescale of the local contribution. The remote process exhibits uniform skill during the CP El Niño events, while the distribution of the remote skill maps geographical variability in the EP El Niño event.

Acknowledgements

References

Ashok, K., Yamagata, T., 2009. The El Niño with a difference. Nature 461, 481–484.
Ashok, K., Behera, S.K., Rao, S.A., Weng, H., Yamagata, T., 2007. El Niño Modoki and its possible teleconnection. Journal of Geophysical Research 112, C11007. http://dx.doi.org/10.1029/2006JC003798.
Balmaseda, M.A., Vidard, A., Anderson, D.L.T., 2008. The ECMWF Ocean Analysis System: ORA-S3. Monthly Weather Review 136, 3018–3034.
Bindoff, N.L., Willebrand, J., Artale, V., Cazenave, A., Gregory, J., Gulev, S., Hanawa, K., Le Quéré, C., Levitus, S., Nojiri, Y., Shum, C.K., Talley, L.D., Unnikrishnan, A., 2007. Observations: oceanic climate change and sea level. In: Solomon, S., Qin, D., Manning, M., Chen, Z., Marquis, M., Averyt, K.B., Tignor, M., Miller, H.L. (Eds.), Climate Change 2007: The Physical Science Basis. Contribution of Working Group I to the Fourth Assessment Report of the Intergovernmental Panel on Climate Change. Cambridge University Press, Cambridge, United Kingdom and New York, NY, USA.
Cai, W.-Y., Lengaigne, M., Borlace, S., Collins, M., Cowan, T., McPhaden, M.J., Timmermann, A., Power, S., Brown, J., Menkes, C., Ngari, A., Vincent, E.M., Widlansky, M.J., 2012. More extreme swings of the South Pacific convergence zone due to greenhouse warming. Nature 488, 365–369.
Cazenave, A., Lombard, A., Llovel, W., 2008. Present-day sea level rise: a synthesis. Comptes Rendus Geosciences 340, 761–770.
Chang, C.-W.J., Hsu, H.-H., Wu, C.-R., Sheu, W.-J., 2008. Interannual mode of sea level in the South China Sea and the roles of El Niño and El Niño Modoki. Geophysical Research Letters 35, L03601. http://dx.doi.org/10.1029/2007GL032562.
Ding, Q., Steig, E.J., Battisti, D.S., Küttel, M., 2011. Winter warming in West Antarctica caused by central tropical Pacific warming. Nature Geoscience 4, 398–403.
Epstein, E.S., 1969. Stochastic dynamic prediction. Tellus 21 (6), 739–759.
Fine, R.A., Lukas, R., Bingham, F.M., Warner, M.J., Gammon, R.H., 1994. The western equatorial Pacific: a water mass crossroads. Journal of Geophysical Research 99, 25063–25080.
Garfinkel, C.I., Hurwitz, M.M., Waugh, D.W., Butler, A.H., 2012. Are the teleconnections of Central Pacific and Eastern Pacific El Niño distinct in boreal wintertime? Climate Dynamic. http://dx.doi.org/10.1007/s00382-012-1570-2.
Gu, X.-L., Li, P.-L., 2009. Pacific sea level variations and its factors. Acta Oceanologica Sinica 31 (1), 28–36.
Kao, H.-Y., Yu, J.-Y., 2009. Contrasting eastern-Pacific and central-Pacific types of ENSO. Journal of Climate 22, 615–632.
Kug, J.-S., Jin, F.-F., An, S.-L., 2009. Two types of El Niño event: Cold Tongue El Niño and Warm Pool El Niño. Journal of Climate 22, 1499–1515.
Lagerloef, G.S.E., 1995. Interdecadal variations in the Alaska Gyre. Journal of Physical Oceanography 25, 2242–2258.
Larson, S., Lee, S.-K., Wang, C., Chung, E.-S., Enfield, D., 2012. Impacts of non-EP El Niño patterns on Atlantic hurricane activity. Geophysical Research Letters 39, L14706. http://dx.doi.org/10.1029/2012GL052595.
Lee, T., McPhaden, M.J., 2010. Increasing intensity of El Niño in the central-equatorial Pacific. Geophysical Research Letters 37, L14603. http://dx.doi.org/10.1029/2010GL044007.
Li, Y.-L., Yu, Y.-Q., Zhang, X.-H., Xiao, W.-N., 2004. Numerical simulation of seasonal cycle and interannual variation of sea surface height in the tropical Pacific and Indian Oceans. Chinese Journal of Atmospheric Science 28 (4), 493–509.
Li, G., Ren, B.-H., Yang, C.-Y., Zhang, J.-Q., 2010. Traditional El Niño and El Niño Modoki revisited: is El Niño Modoki linearly independent of traditional El Niño. Atmospheric and Oceanic Science Letters 3, 70–74.
Li, Y.-F., Zuo, J.-C., Li, J., Chen, M.-X., 2012. The influence of wind anomaly on tropical Pacific sea level variation during El Niño. Acta Oceanologica Sinica 42, 1–7.
Llovel, W., Guinehut, S., Cazenave, A., 2010. Regional and interannual variability in sea level over 2002–2009 based on satellite altimetry, Argo float data and GRACE ocean mass. Ocean Dynamics 60, 1193–1204.
Llovel, W., Becker, M., Cazenave, A., Jevrejeva, S., Alkama, R., Decharme, B., Douville, H., Ablain, M., Beckley, B., 2011. Terrestrial waters and sea level variations on interannual time scale. Global and Planetary Change 75, 76–82.
Lukas, R., Firing, E., Hacker, P., Richardson, P.L., Collins, C.A., Fine, R., Gammon, R., 1991. Observations of the Mindanao Current during the Western Equatorial Pacific Ocean Circulation Study. Journal of Geophysical Research 96, 7089–7104.
Nerem, R.S., Chambers, D.P., Choe, C., Mitchum, G.T., 2010. Estimating mean sea level change from the TOPEX and Jason altimeter missions. Marine Geodesy 33, 435–446.
Qiu, B., 2002. Large-scale variability in the midlatitude subtropical and subpolar North Pacific Ocean, observations and causes. Journal of Physical Oceanography 32, 353–375.
Qiu, B., Chen, S., 2010. Interannual-to-decadal variability in the bifurcation of the North Equatorial Current off the Philippines. Journal of Physical Oceanography 40, 2525–2538.
Stammer, D., 1997. Steric and wind-induced changes in TOPEX/POSEIDON large-scale sea surface topography observations. Journal of Geophysical Research 102, 20987–21009.
Tian, H., Zhou, T.-H., Chen, Z.-Y., 1993. A stochastic dynamical prediction model of mean sea level changes. Journal of Ocean University of Qingdao 23 (1), 33–42.
Wang, C.-Z., Fiedler, P.C., 2006. ENSO variability in the eastern tropical Pacific: a review. Progress in Oceanography 69, 239–266.
Weng, H., Ashok, K., Behera, S.K., Rao, S.A., Yamagata, T., 2007. Impacts of recent El Nino Modoki on dry/wet conditions in the Pacific rim during boreal summer. Climate Dynamics 29, 113–129.
Willis, J.K., Chambers, D.P., Nerem, R.S., 2008. Assessing the globally averaged sea level budget on seasonal to interannual timescales. Journal of Geophysical Research 113, C06015. http://dx.doi.org/10.1029/2007JC004517.
Wyrtki, K., 1989. Some thoughts about the West Pacific Poo1. Proceedings of the Western Pacific International Meeting and Workshop on Yoga-Coare, Orstom, Noumea, New Caledonia, pp. 99–109.
Xu, S.-S., Zuo, J.-C., Chen, M.-X., 2010. North Pacific sea level change and its impact factors during 1993–2006. Acta Oceanologica Sinica 40, 24–32.
Zhang, X., Church, J.A., 2012. Sea level trends, interannual and decadal variability in the Pacific Ocean. Geophysical Research Letters 39, L21701. http://dx.doi.org/10.1029/2012GL053240.